Research Article GU J Sci, Part A, 9(4): 545-553 (2022) https://doi.org/10.54287/gujsa.1205356

Gazi University
Journal of Science
PART A: ENGINEERING AND INNOVATION
http://dergipark.org.tr/gujsa

A Computational Study of the Adsorptive Separation of Methane and Hydrogen in Zeolite Templated Carbons

Celal Utku DENİZ[1*]

[1]*Hitit University, Faculty of Engineering, Department of Chemical Engineering, 19030, Çorum, Türkiye*

Keywords

Hydrogen
Methane
Gas Separation
GCMC
Zeolite Templated Carbons

Abstract

Combustion of conventional energy sources produces pollutants such as SO_x, NO_x, and CO; the use of hydrogen and methane can eliminate these harmful emissions. In fuel cell technology and other uses, hydrogen must be refined by extracting methane from the methane/hydrogen combination, produced via dry or steam reforming. This study investigates the adsorption and separation capabilities of recently discovered zeolite-templated carbons (ZTCs) for binary mixtures consisting of hydrogen and methane. To assess the adsorption and separation performances of these carbon-based nanostructures, grand canonical Monte Carlo (GCMC) simulations were used. The simulation results revealed that AFY ($|(C_6H_{15}N)_3(H_2O)_7|[Co_3Al_5P_8O_{32}]$) and RWY ($|(C_6H_{18}N_4)_{16}|$ $[Ga_{32}Ge_{16}S_{96}]$) structures could be viable alternatives for applications involving adsorptive gas separation based on selectivity and the CH_4 uptake capacity. The selectivity of AFY was calculated to be 176, while its capacity to uptake CH_4 was found to be 2.57 mmol/g, the selectivity of RWY was calculated to be 132, and its CH_4 uptake was 3.49 mmol/g.

Cite

Deniz, C. U. (2022). A Computational Study of the Adsorptive Separation of Methane and Hydrogen in Zeolite Templated Carbons. *GU J Sci, Part A, 9*(4), 545-553.

Author ID (ORCID Number)

C. U. Deniz, 0000-0003-0948-9626

Article Process

Submission Date 16.11.2022
Revision Date 24.11.2022
Accepted Date 29.11.2022
Published Date 31.12.2022

1. INTRODUCTION

Compared to traditional energy sources, which create pollutants during combustion (such as SO_x, NO_x, CO, etc.), hydrogen and methane are more desirable options. Dry reforming and steam reforming processes are used in industry to produce hydrogen. In some applications, such as fuel cell technology, the hydrogen must be purified by separating methane from the methane/hydrogen mixture. Cryogenic distillation and chemical adsorption, two traditional methods for separating gases, have drawbacks such as high costs, poor safety, and difficult operating conditions (Niaz et al., 2015). Gas adsorption/separation using porous materials has recently been identified as a possible solution (Li et al., 2022).

Various porous adsorbents, including covalent organic materials, zeolites, and metal-organic materials, have been proposed for gas storage applications (Zhang et al., 2013). Currently, these materials have demonstrated highly promising storage performance for pure gases. In contrast, most industrial processes involve gas mixtures instead of pure gases. Consequently, evaluating these materials' mixed gas adsorption performance is crucial. Evaluating the adsorption characteristics of gas mixtures indicates the selectivity of the adsorbent and, thus, its applicability in adsorptive gas separation for various applications (Kosinov et al., 2016).

The principle behind the adsorptive separation of gas mixtures is the selective adsorption of a component on the adsorbent compared to the others. The selectivity is determined by several factors, such as the adsorbent and the adsorbate molecule interaction, the pore size of the adsorbent, and the geometry of the molecule being adsorbed. A high specific surface area is a crucial parameter for adsorption capacity, but a pore size that

*Corresponding Author, e-mail: cutkudeniz@hitit.edu.tr

matches the diameter of one of the gas mixture components can improve the framework's interaction with that molecule. In such a system, the framework selectively adsorp some molecules and reject others. Activated carbons, polymers, and metal-organic materials are a few of the adsorbents proposed for adsorptive gas separation applications (Attia et al., 2020).

Using numerical analysis methods, carbon-based nanostructures' single-gas storage capacities have been widely explored (Ozturk et al., 2015; Mert et al., 2020). However, there is limited research on gas mixtures' separation performance in the literature. Majumdar et al. (2018) employed the GCMC method to study the adsorptive separation of CO_2 from H_2S, SO_2, and N_2 multicomponent gas combinations in carbon nanotube arrays. Sha and Faller (2016) employed GCMC simulations to assess the carbon-based nanostructures in the separation performance of pure noble gases. GCMC and molecular dynamic simulations are used by Wang and Cao (2015) to evaluate the separation capabilities of the covalent organic frameworks (COFs) for binary mixtures of H_2S, N_2, CO_2, CH_4, SO_2, and CO_2 gases.

Zeolite-templated carbons (ZTCs) were developed from the concept of creating microporous carbon-based materials with a porosity similar to that of the original zeolite templates. Their substantial specific surface area and distinctive microporous structure can make them effective gas adsorbents. Furthermore, ZTCs can be produced in large amounts effectively (Nishihara & Kyotani, 2018). Recent work by Braun et al. (2018) provided an analytical groundwork for obtaining a ZTC starting from a zeolite, outlined the basics of forming ZTCs, and discovered 68 ZTCs. As previously indicated, even though ZTCs have a very high potential for use as an adsorbent in gas storage applications (Deniz, 2022), there has been no research on how effectively these structures separate methane and hydrogen gas mixture.

Motivated by these facts, adsorptive separation performances of the zeolite-templated carbons identified by Braun et al. (2018) are investigated for the hydrogen/methane equimolar mixture. The efficiency of methane/hydrogen separation is evaluated employing the grand canonical Monte Carlo (GCMC) approach. In order to interpret the results, selectivity and the differential enthalpy of adsorption (ΔH_{Ads}) were used along with the structural parameters of the ZTCs. According to the findings of the simulations, some of the ZTCs has the potential as a promising option for applications involving adsorptive gas separation.

2. MATERIAL AND METHOD

The GCMC simulations for adsorption and separation were run with the RASPA molecular simulation software tool (Dubbeldam et al., 2016). The simulations were run for $2x10^5$ iterations, the first 10^5 of which were utilized to achieve system equilibrium and the second 10^5 to ensure statistical reproducibility. The results showed that further increasing the number of cycles had a minimal impact on findings. Four types of Monte Carlo (MC) move, including swap, reinsertion, translation, and identity change, were considered for simulations. All simulation results were obtained between 0.1 and 100 kPa pressure and a temperature of 298 K.

Lorentz-Berthelot combining approach given in Eqs. 1 and 2 were used to calculate the interactions between individual species. Attraction and repulsion forces between gas molecules and ZTCs were modeled using the Lennard Jones (LJ) potential given in Eq 3, and the electrostatic interactions were also considered employing the Ewald summation.

$$\varepsilon_{ij} = \sqrt{\varepsilon_i \varepsilon_j} \tag{1}$$

$$\sigma_{ij} = \frac{1}{2}\left(\sigma_i + \sigma_j\right) \tag{2}$$

$$U_{ij} = 4\varepsilon_{ij}\left[\left(\frac{\sigma_{ij}}{r_{ij}}\right)^{12} - \left(\frac{\sigma_{ij}}{r_{ij}}\right)^{6}\right] + \frac{q_i q_j}{4\pi\varepsilon_0 r_{ij}} \tag{3}$$

where interacting species are *i* and *j*, the representative distance between species is expressed with σ_{ij} while the potential of the interactions is denoted as ε_{ij}. The distance between species *i* and *j* is denoted by r_{ij}; ε_0 is the dielectric constant, and partial charges for species *i* and *j* are expressed as q_i and *qj*, respectively.

Carbon-Carbon interactions in ZTC structure are considered sp2-hybridized, and suitable potential parameters were selected from the literature (Lithoxoos et al., 2010) and employed in simulations. A rigid spherical model was used to represent hydrogen molecules with a fixed hydrogen bond length (0.74 Å), and the potential parameters reported by Michels et al. (1960) were used. The united-atom model (Peng et al., 2010) was adopted and used in simulations for the methane molecule. Parameters for the potentials in the GCMC simulations are given in Table 1.

Table 1. *The LJ parameters of framework and adsorbate molecules*

Molecule	Reference Study	σ (Å)	ε (K)
C – C (Framework)	(Lithoxoos et al., 2010)	3.40	28.2
H_2	(Michels et al., 1960)	2.96	36.7
CH_4	(Peng et al., 2010)	3.81	148.2

To save computing costs, it was assumed that ZTC frameworks were static. This was also the case in earlier studies (Ozturk et al., 2015). Additionally, periodic boundary conditions were also imposed. After a spherical cutoff of 12.8 Å, the LJ interactions were neglected. The differential enthalpy of adsorption (ΔH_{Ads}), a numerical indicator for adsorption strength between gas molecules and adsorbent, was determined using the energy/particle fluctuations (Vlugt et al., 2008).

Selectivity is utilized to measure the performance of the frameworks in adsorbing hydrogen and methane during the computational gas separation process. Eq. (4) describes the selectivity parameter.

$$S = \frac{X_{H_2} Y_{CH_4}}{X_{CH_4} Y_{H_2}} \tag{4}$$

where S represents the selectivity, X_{H_2} and X_{CH_4}represent the molar adsorption amount of adsorbate molecule species in the adsorption phase, and Y_{H_2} and Y_{CH_4} indicate the concentrations of adsorbate molecule species in the bulk phase, respectively.

Density, specific surface area (SSA), and accessible pore volume (APV) were computed for the ZTC structures using a visualization package called iRASPA (Dubbeldam et al., 2018). Pore-size distribution (PSD) was also determined using RASPA for the chosen ZTC structures (Dubbeldam et al., 2016). In this study, when naming ZTC structures, original zeolite-template code names were used.

3. RESULTS AND DISCUSSION

Selectivity is one of the most important metrics for assessing the gas separation capability of nanostructures. Consequently, the selectivity of ZTC structures considered within the scope of this study is evaluated, and a more detailed assessment based on APV, SSA, pore-size distribution, and adsorption isotherm is carried out on selected ZTC structures following the initial assessment. First, the CH_4/H_2 selectivities of 68 ZTCs are estimated at 298 K and 100 kPa conditions to determine the most promising ZTC structures for methane/hydrogen adsorptive separation. The selectivities of the ZTC structures are given in Figure 1.

As seen in Figure 1, AFY, BOG ($(|Ca_7Na_4(H_2O)_{74}|[Al_{18}Si_{78}O_{192}])$), JSR_1 ($|(Ni(C_3H_{10}N_2)_3)_{36}Ni_{4.7}|_3[Ga_{27.1}Ge_{68.9}O_{192}]_3$), JSR_3, and RWY structures differ in selectivity. The selectivities for AFY, BOG, JSR_1, JSR_3, and RWY structures were calculated as 176, 95, 93, 97, and 132, respectively. In the following parts of the study, a detailed examination of these structures will be carried out. In this context, calculated densities, APV, and SSA of the promising structures are given in Table 2. The representative structures are also given in Figure 2.

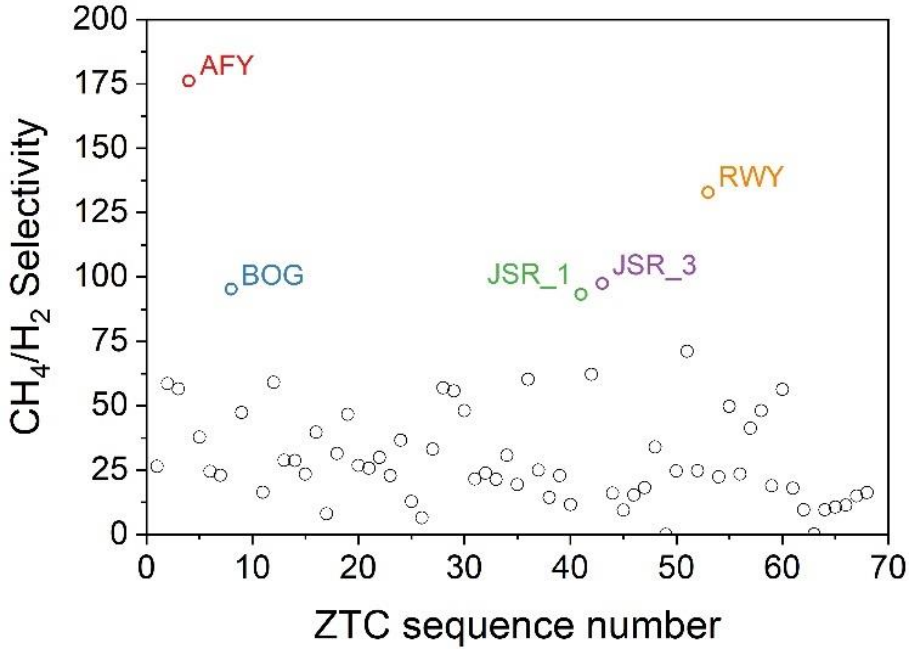

Figure 1. *Selectivity of 68 ZTCs at 298K and 100 kPa*

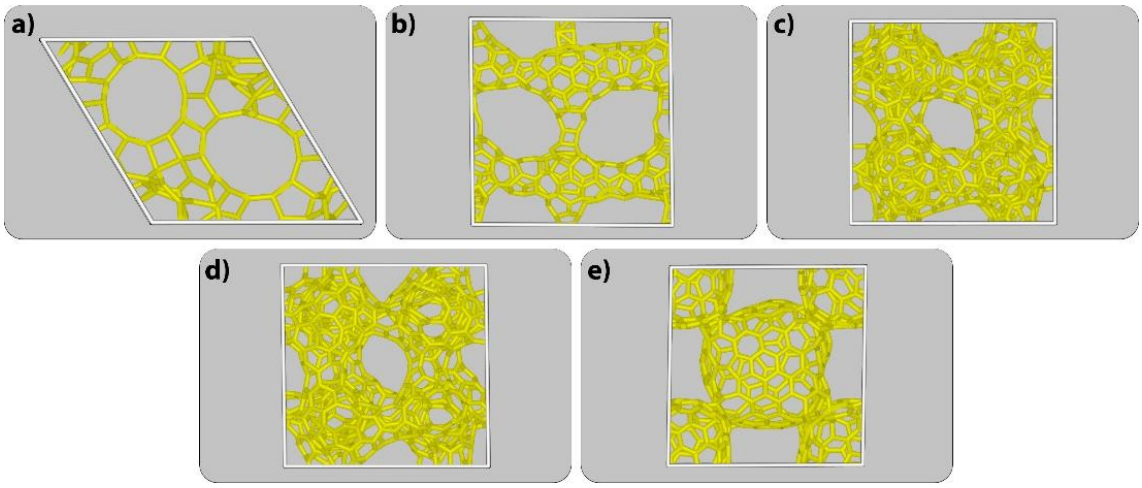

Figure 2. *The representative structures of* ***a)*** *AFY* ***b)*** *BOG* ***c)*** *JSR_1* ***d)*** *JSR_3* ***e)*** *RWY*

When Table 2 is examined, it can be said that the RWY structure has a lower density and higher surface area than the others. On the other hand, it is expected that the BOG, JSR_1, and JSR_3 structures would exhibit comparable adsorption characteristics due to the similarities between their SSA and APV.

Table 2. *Structural properties of ZTCs*

Structure	SSA (m^2/g)	APV (cm^3/g)	Density (g/cm^3)
AFY	1107.7	0.5033	1.432
BOG	1018.9	0.3843	1.406
JSR_1	953.7	0.4408	1.489
JSR_3	893.2	0.4186	1.514
RWY	1681.3	0.7620	1.233

The pore size of carbon-based nanomaterials (CBNs) is critical in determining their adsorption performance. Figure 3 displays the PSDs for the AFY, BOG, JSR_1, JSR_3, and RWY structures, and only micropores exist in the specified ZTC structures. The gas storage ability of CBNs is known to be poor if their pores are smaller than 5 Å (Mert et al., 2020). Notably, the selected ZTC structures all have pore sizes that fall within the range of what is considered an appropriate pore size for adsorbents (Deniz, 2022), with the smallest pore size being around 2 Å and the largest being around 8 Å.

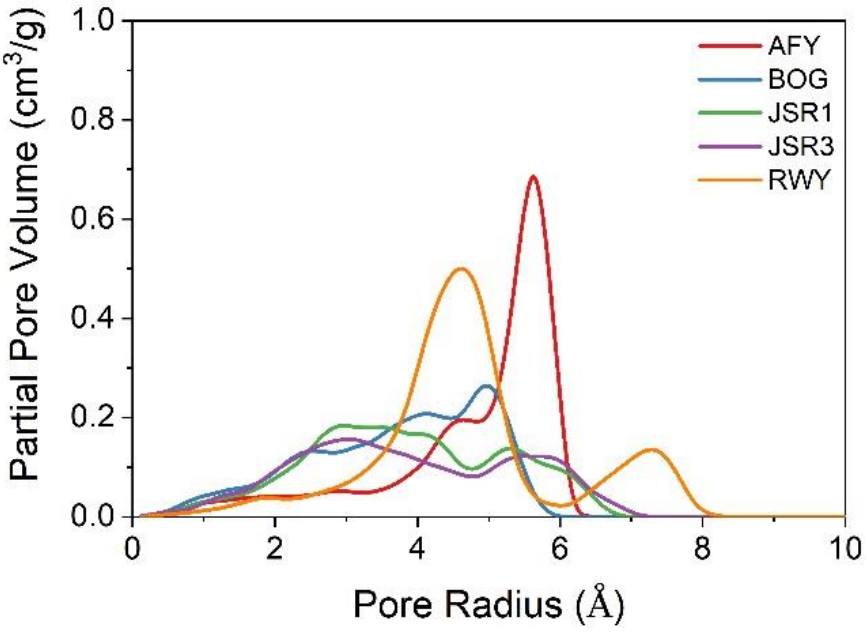

Figure 3. *Pore size distribution of ZTC structures*

Figure 4a shows that H_2 uptake capabilities grow linearly with increasing pressure from 0.1 to 100 kPa at 298 K. Hydrogen adsorption capacity of five ZTCs is shown to be more closely related to pore volume than surface area and ΔH_{Ads} at 298 K, as shown by the highly linear isotherms. According to Table 2 and Figure 4a, the order of the APV and hydrogen adsorption capacity of five ZTCs is RWY > AFY > JSR_1 > JSR_3 > BOG. Furthermore, the pore size distribution seen in Figure 3 can be used to justify RWY and AFY storing more H_2 as pressure increases. Considering that the kinetic diameter of hydrogen molecules is around 2.89 Å (Dal-Cin et al., 2008), it can be stated that these two structures with larger pores and sharper distribution establish better contact with the surface and increase their surface area. On the other hand, JSR_1, JSR_3, and BOG structures have relatively small pores to enhance the surface area. Figure 4b also shows the ΔH_{Ads} of ZTCs. From the perspective of gas separation performance, it is advantageous that the ΔH_{Ads} of hydrogen for ZTCs are less than 15 kJ/mol, which is regarded as an appropriate value for hydrogen adsorption in porous materials (van den Berg & Areán, 2008).

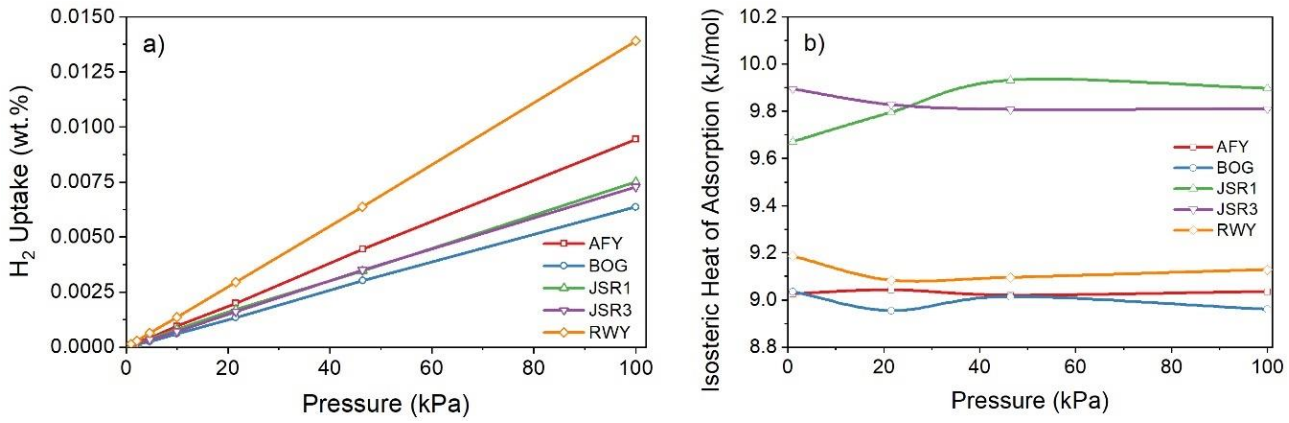

Figure 4. a) *H_2 uptake capacities and* ***b)*** *ΔH_{Ads} values*

Figure 5a depicts the adsorption isotherms, while Figure 5b shows ΔH_{Ads} of methane in ZTCs at 298 K. The non-linear pressure-dependency of CH_4 adsorption capacity is visible in Figure 5a at 298 K. This is a distinct trend from that observed in Figure 4a for H_2 uptake capacity at 298 K. This indicates the fact that at 298 K, five ZTCs can adsorp enough methane to reach saturation, and it is due to the higher adsorption affinity of CH_4 relative to H_2. The comparatively limited pore volume of JSR_1, JSR_3, and BOG, results in the CH_4 adsorption capabilities at low pressure being close to saturation. For 100 kPa and 298 K, the CH_4 adsorption capacities of AFY, BOG, JSR_1, JSR_3, and RWY are 4.13, 2.34, 2.74, 2.45, and 5.59 wt.%, respectively. Comparing Figure 4b and Figure 5b, one can conclude that the ΔH_{Ads} for CH_4 (23.4–26 kJ/mol) in five ZTCs are significantly higher compared to H_2 (9–10 kJ/mol). Similar ΔH_{Ads} values have also been reported by Li et al. (2022) for covalent organic frameworks. In this context, these ZTCs have the potential to effectively separate CH_4/H_2 mixtures according to their higher adsorption capacity and ΔH_{Ads} for CH_4.

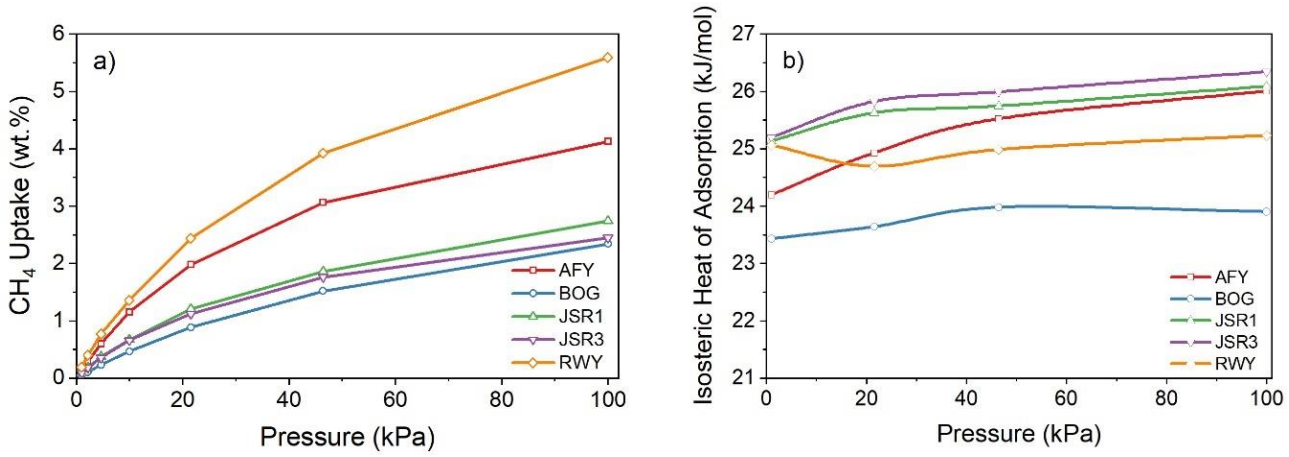

Figure 5. a) *CH_4 uptake capacities and* ***b)*** *ΔH_{Ads} values*

The adsorption selectivity of ZTCs at 298 K is evaluated for different pressures considering the binary mixture of CH_4 and H_2 with the same molar ratio. Figure 6 depicts the influence of pressure (0.1–100 kPa) on selectivity at a constant temperature. As shown in Figure 6, the selectivity of all structures decreases with increasing pressure. For the 100 kPa and 298 K conditions, the CH_4/H_2 selectivities of AFY, BOG, JSR_1, JSR_3, and RWY were calculated as 176, 95, 93, 97, and 132, respectively.

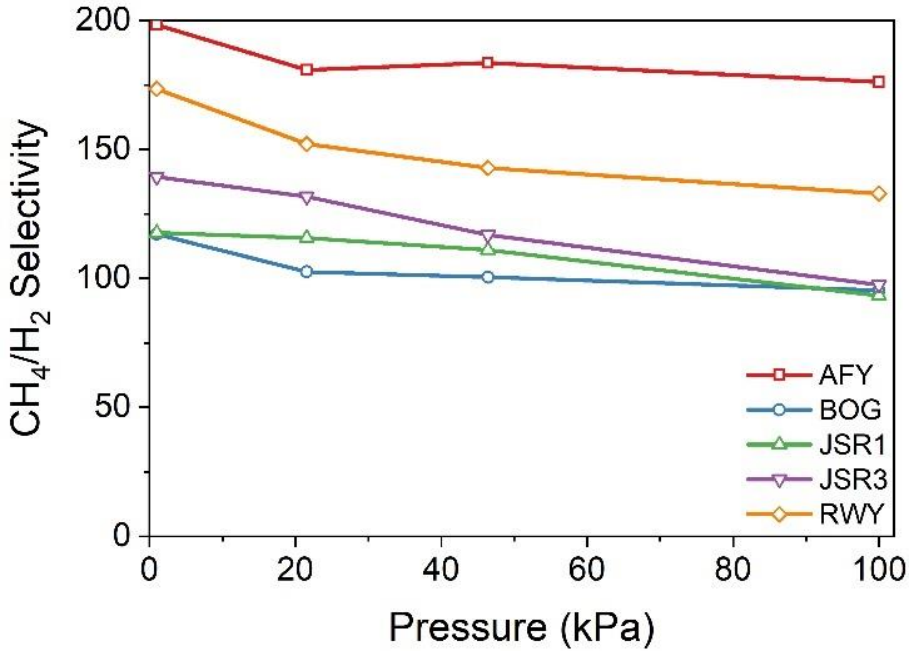

Figure 6. *Effect of pressure on CH_4/H_2 selectivity of ZTC structures*

Numerous aspects must be considered to understand the dependency of selectivity on pressure, such as the structural properties of ZTCs, the diameter of adsorbates, and the ΔH_{Ads} for adsorbates in the host material. It can be observed in Figure 4b and 5b that CH_4 has higher ΔH_{Ads} in ZTCs than H_2, allowing it to interact with the frameworks more strongly than H_2. As a result, the CH_4 to H_2 ratio is always higher than 1. Under mild pressure, adsorbates interact with the host material and are primarily adsorbed on the framework surface. Therefore, the methane/hydrogen selectivity is quite strong at low pressures because CH_4 has an even greater ΔH_{Ads} than H_2. When the pressure increases, the gas molecules are started to spread out throughout the framework and cover its accessible surface completely. In this instance, because of the difference in molecule size between hydrogen (2.89 Å) and methane (3.8 Å) (Dal-Cin et al., 2008), hydrogen can reach places that methane cannot; hence the selectivity between the two gases begins to decrease.

The performance of CH_4/H_2 separation is primarily determined by two factors: selectivity and methane uptake capability. AFY (Selectivity: 176 and CH_4 Uptake: 2.57 mmol/g) and RWY (Selectivity: 132 and CH_4 Uptake: 3.49 mmol/g) are more suitable compared to BOG, JSR_1, and JSR_3 for separating methane from the mixture.

In the literature, different researchers have used different temperature and pressure conditions when calculating selectivity and methane uptake capacity. For this reason, unfortunately, most of the data in the literature are not comparable with each other. However, a comparison was made with the data in the literature obtained under similar working conditions. Zhou et al. (2017) reported that a recently synthesized metal-organic framework had a selectivity value of about 206 under the same conditions as in this study and a CH_4 storage capacity of approximately 1.1 mmol/g. Li et al. (2022) described that the CH_4/H_2 selectivity for borophosphonate-based covalent organic frameworks (BP-COFs) was about 120 and CH_4 storage capacity was about 4 mmol/g under 100 kPa at 298 K. Yuan et al. (2021) reported that the CH_4/H_2 selectivity for hybrid ultra-microporous materials was about 90 for the same conditions, and the CH_4 uptake was 1.6 mmol/g. As it is understood in the studies in the literature, materials with high selectivity offer low CH_4 storage capacity, and materials with high CH_4 storage properties offer low selectivity.

When the results are compared with previous studies in terms of ΔH_{Ads}, it is seen that the values calculated for methane (23.4–26 kJ/mol) and hydrogen (9–10 kJ/mol) are consistent with previous studies in the literature. For instance, Zhou et al. (2017) noted these values as 24 - 27 kJ/mol for methane and about 9 kJ/mol for hydrogen. Similarly, Li et al. (2022) reported ΔH_{Ads} for hydrogen (9 - 10 kJ/mol) and (14 - 26 kJ/mol) for methane in BP-COFs structures. It should be noted here that the selectivity of the material, with the low ΔH_{Ads} (14 kJ/mol), is also relatively low (about 10). When materials are evaluated in terms of ΔH_{Ads}, it can be said that to achieve high CH_4/H_2 selectivity and high methane storage together, it should be as low as possible for hydrogen and vice versa for methane. Today's economic materials are, unfortunately, somewhat limited in this respect. Moreover, it seems unlikely that this can be achieved only with the structural properties of materials such as SSA and APV. It may be possible to overcome this limitation by identifying and incorporating functional groups with high methane and low hydrogen affinity into the structures. All these results reveal that the AFY and RWY structures are comparable with the materials in the literature for adsorbing methane from the mixture and can be used for purifying hydrogen or capturing methane.

4. CONCLUSION

In this work, ZTC structures that were recently discovered were investigated for their potential use as an adsorbent in an application involving the separation of methane and hydrogen. First, there were 68 ZTCs initially; however, this number was cut down to five so that they could be investigated in greater depth, taking into account their selectivity performance. GCMC method was employed to assess the adsorptive separation capabilities of the ZTCs for methane and hydrogen mixture. Depending on the results, five ZTCs offer favorable characteristics for separating methane/hydrogen gas mixture, including a large APV (0.38 - 0.76 cm^3/g), an appropriate pore size distribution (2 - 8 Å), and a specific surface area (893 - 1681 cm^2/g). At ambient temperature, the GCMC simulation reveals that the ZTCs can adsorp a more significant amount of CH_4 than H_2. The separation simulations demonstrate that AFY and RWY are more suited for adsorbing methane from the mixture in terms of selectivity and methane uptake capacity. The performance of five ZTCs in gas adsorption and separation is comprehensively related to structural factors such as APV, SSA, and PSD,

and the pressure also influences it. According to the findings of this research, ZTC structures, especially AFY and RWY, are potentially applicable host materials for the purpose of separating methane and hydrogen.

CONFLICT OF INTEREST

The author declares no conflict of interest.

REFERENCES

Attia, N. F., Jung, M., Park, J., Jang, H., Lee, K., & Oh, H. (2020). Flexible nanoporous activated carbon cloth for achieving high H_2, CH_4, and CO_2 storage capacities and selective CO_2/CH_4 separation. *Chemical Engineering Journal*, *379*, 122367. doi:10.1016/j.cej.2019.122367

Braun, E., Lee, Y., Moosavi, S. M., Barthel, S., Mercado, R., Baburin, I. A., Proserpio, D. M., & Smit, B. (2018). Generating carbon schwarzites via zeolite-templating. *Proceedings of the National Academy of Sciences of the United States of America*, *115*(35), E8116-E8124. doi:10.1073/pnas.1805062115

Dal-Cin, M. M., Kumar, A., & Layton, L. (2008). Revisiting the experimental and theoretical upper bounds of light pure gas selectivity–permeability for polymeric membranes. *Journal of Membrane Science*, *323*(2), 299-308. doi:10.1016/j.memsci.2008.06.027

Deniz, C. U. (2022). Computational screening of zeolite templated carbons for hydrogen storage. *Computational Materials Science*, *202*, 110950. doi:10.1016/j.commatsci.2021.110950

Dubbeldam, D., Calero, S., Ellis, D. E., & Snurr, R. Q. (2016). RASPA: Molecular simulation software for adsorption and diffusion in flexible nanoporous materials. *Molecular Simulation*, *42*(2), 81-101. doi:10.1080/08927022.2015.1010082

Dubbeldam, D., Calero, S., & Vlugt, T. J. H. (2018). iRASPA: GPU-accelerated visualization software for materials scientists. *Molecular Simulation*, *44*(8), 653-676. doi:10.1080/08927022.2018.1426855

Kosinov, N., Gascon, J., Kapteijn, F., & Hensen, E. J. M. (2016). Recent developments in zeolite membranes for gas separation. *Journal of Membrane Science*, *499*, 65-79. doi:10.1016/j.memsci.2015.10.049

Li, X.-D., Yang, P., Huang, X.-Y., Liu, X.-Y., Yu, J.-X., & Chen, Z. (2022). Computational simulation study on adsorption and separation of CH4/H2 in five higher-valency covalent organic frameworks. *Materials Today Communications*, *33*, 104374. doi:10.1016/j.mtcomm.2022.104374

Lithoxoos, G. P., Labropoulos, A., Peristeras, L. D., Kanellopoulos, N., Samios, J., & Economou, I. G. (2010). Adsorption of N2, CH4, CO and CO2 gases in single walled carbon nanotubes: A combined experimental and Monte Carlo molecular simulation study. *Journal of Supercritical Fluids*, *55*(2), 510-523. doi:10.1016/j.supflu.2010.09.017

Majumdar, S., Maurya, M., & Singh, J. K. (2018). Adsorptive Separation of CO2 from Multicomponent Mixtures of Flue Gas in Carbon Nanotube Arrays: A Grand Canonical Monte Carlo Study. *Energy & Fuels*, *32*(5), 6090-6097. doi:10.1021/acs.energyfuels.8b00649

Mert, H., Deniz, C. U., & Baykasoglu, C. (2020). Monte Carlo simulations of hydrogen adsorption in fullerene pillared graphene nanocomposites. *Molecular Simulation*, *46*(8), 650-659. doi:10.1080/08927022.2020.1758696

Michels, A., de Graaff, W., & Ten Seldam, C. A. (1960). Virial coefficients of hydrogen and deuterium at temperatures between −175°C and +150°C. Conclusions from the second virial coefficient with regards to the intermolecular potential. *Physica*, *26*(6), 393-408. doi:10.1016/0031-8914(60)90029-X

Niaz, S., Manzoor, T., & Pandith, A. H. (2015). Hydrogen storage: Materials, methods and perspectives. *Renewable and Sustainable Energy Reviews*, *50*, 457-469. doi:10.1016/j.rser.2015.05.011

Nishihara, H., & Kyotani, T. (2018). Zeolite-templated carbons-three-dimensional microporous graphene frameworks. *Chemical Communications*, *54*(45), 5648-5673. doi:10.1039/c8cc01932k

Ozturk, Z., Baykasoglu, C., Celebi, A. T., Kirca, M., Mugan, A., & To, A. C. (2015). Hydrogen storage in heat welded random CNT network structures. *International Journal of Hydrogen Energy, 40*(1), 403-411. doi:10.1016/j.ijhydene.2014.10.148

Peng, X., Zhou, J., Wang, W., & Cao, D. (2010). Computer simulation for storage of methane and capture of carbon dioxide in carbon nanoscrolls by expansion of interlayer spacing. *Carbon, 48*(13), 3760-3768. doi:10.1016/j.carbon.2010.06.038

Sha, H., & Faller, R. (2016). Molecular simulation of adsorption and separation of pure noble gases and noble gas mixtures on single wall carbon nanotubes. *Computational Materials Science, 114*, 160-166. doi:10.1016/j.commatsci.2015.12.031

van den Berg, A. W. C., & Areán, C. O. (2008). Materials for hydrogen storage: current research trends and perspectives. *Chemical Communications, 6*, 668-681. doi:10.1039/B712576N

Vlugt, T. J. H., García-Pérez, E., Dubbeldam, D., Ban, S., & Calero, S. (2008). Computing the Heat of Adsorption using Molecular Simulations: The Effect of Strong Coulombic Interactions. *Journal of Chemical Theory and Computation, 4*(7), 1107-1118. doi:10.1021/ct700342k

Wang, H., & Cao, D. (2015). Diffusion and Separation of H2, CH4, CO2, and N2 in Diamond-Like Frameworks. *The Journal of Physical Chemistry C, 119*(11), 6324-6330. doi:10.1021/jp512275p

Yuan, J., Liu, X., Li, X., & Yu, J. (2021). Computer simulations for the adsorption and separation of CH4/H2/CO2/N2 gases by hybrid ultramicroporous materials. *Materials Today Communications, 26*, 101987. doi:10.1016/j.mtcomm.2020.101987

Zhang, Q., Uchaker, E., Candelaria, S. L., & Cao, G. (2013). Nanomaterials for energy conversion and storage. *Chemical Society Reviews, 42*(7), 3127-3171. doi:10.1039/C3CS00009E

Zhou B., Li W., & Zhang J. (2017). *The Journal of Physical Chemistry C*, *121*(37), 20197-20204. doi:10.1021/acs.jpcc.7b07108